



Construction of protein-modified TiO₂ nanoparticles for use with ultrasound irradiation in a novel cell injuring method

Chiaki Ogino^{a,b}, Naonori Shibata^a, Ryosuke Sasai^a, Keiko Takaki^b, Yusuke Miyachi^{a,d}, Shun-ichi Kuroda^c, Kazuaki Ninomiya^b, Nobuaki Shimizu^{a,b,*}

^a The Division of Material Sciences, Graduate School of Natural Science and Technology, Kanazawa University, Kakuma, Kanazawa 920 1192, Japan

^b Institute of Nature and Environmental Technology, Kanazawa University, Kakuma, Kanazawa 920 1192, Japan

^c Department of Structural Molecular Biology, The Institute of Scientific and Industrial Research (ISIR), Osaka University, Mihogaoka 8-1, Ibaraki, Osaka 567 0047, Japan

^d Department of Chemical Science and Engineering, Graduate School of Engineering, Kobe University, Rokkoudaichou, Nada-ku, Kobe 657 8501, Japan

ARTICLE INFO

Article history:

Received 26 March 2010

Revised 21 June 2010

Accepted 23 June 2010

Available online 1 July 2010

Keywords:

TiO₂ nanoparticle

Hepatitis B virus

Drug delivery system

Ultrasound irradiation

OH radical

ABSTRACT

Recently, our group discovered an alternative titanium dioxide (TiO₂) activation method that uses ultrasound irradiation (US/TiO₂) instead of ultraviolet irradiation. The pre-S1/S2 protein from hepatitis B virus, which recognizes liver cells, was immobilized to the surface of TiO₂ nanoparticles using an amino-coupling method. The ability of the protein-modified TiO₂ nanoparticles to recognize liver cells was confirmed by surface plasmon resonance analysis and immuno-staining analyses. After uptake of TiO₂ nanoparticles by HepG2 cancer cells, the cells were injured using this US/TiO₂ method; significant cell injury was observed at an ultrasound irradiation intensity of 0.4 W/cm². Together with these results, this strategy could be applied to new cell injuring systems that use ultrasound irradiation in place of photodynamic therapy in the near future.

© 2010 Elsevier Ltd. All rights reserved.

Titanium dioxide (TiO₂) is a photocatalyst and reactive oxygen species (ROS) can be generated on the surface of TiO₂ by ultraviolet irradiation ($\lambda < 390$ nm).^{1,2} Because ROS strongly catalyze reactions that result in degradation of many harmful chemicals, the killing of microorganisms,^{3,4} and injury of mammalian cells,^{5,6} TiO₂ has been used as a photocatalyst in sanitization processes to maintain clean environments in hospitals.⁷ Recently, our group discovered an alternative TiO₂-activation method that uses ultrasound irradiation (US/TiO₂) instead of ultraviolet irradiation.⁸ The US/TiO₂ method produced an OH radical upon combination with methylene blue—a typical substrate for photocatalytic reactions—and other various radical scavengers. Although ultrasound irradiation in aqueous media is known to produce various ROS, including OH radicals and superoxide anion oxygen radicals (O₂⁻), it was assumed that production of ROS, including OH radicals, was enhanced using the US/TiO₂ method. Furthermore, production of ROS using the US/TiO₂ method with pellet-type TiO₂, such as ceramics, had been previously applied to chemical degradation^{8–10} and to killing microorganisms such as an *Escherichia coli*^{11,13} and *Legionella* strains.¹² The advantage of the US/TiO₂ method over the typical photo-excitation and ultraviolet irradiation methods is that it can be used on non-transparent media. Because sound waves generated by ultrasound can

transmit through non-transparent media, TiO₂ located within non-transparent media, such as the human body, can be activated by ultrasound, but not by photo-excitation or ultraviolet radiation.

Photodynamic therapy (PDT) is well-known as a novel approach to cancer treatment based on the produced ROS. Typical PDT is carried out using the combination of a photosensitizer, such as porphyrin IX, and an activator, typically a laser. PDT works by producing ROS that result in cell injury or death. However, the application of PDT is limited to the laser-irradiated area, so the clinical use of PDT has been restricted to cases of skin cancer.^{14,15}

Because the ROS generated on the surface of TiO₂ have very short half-lives,¹⁶ a large portion of the ROS disappear during diffusion in aqueous media without participating in any cell injuring or killing. Therefore, delivery of TiO₂ nanoparticles to specific target tissues is required for effective cell injuring using the US/TiO₂ method. However, TiO₂ has no cell-recognition potential. Moreover, the OH residues on the surface of TiO₂ nanoparticles easily associate with each other at neutral pH, resulting in aggregation of nanoparticles.¹⁷ After aggregation occurs, the nanoparticles are no longer able to transfer into blood and therefore have no adaptation to clinical utility. Sonezaki et al. constructed TiO₂ nanoparticles that remained in suspension at neutral pH by surface modification of the nanoparticles with polyacrylic acid (PAA) at high temperature.¹⁸ Because the dissociation constant of the carboxylic acid group of PAA is approximately pK_a = 4.0,¹⁹ the carboxylic acid group of PAA can dissociate

* Corresponding author. Tel.: +81 76 234 4807; fax: +81 76 234 4829.

E-mail address: nshimizu@t.kanazawa-u.ac.jp (N. Shimizu).

into anionic ion in neutral pH solution, and these electric charge assist of stable formation of TiO₂ nanoparticle. In addition, the carboxylic acid group of PAA allows an immobilization of proteins to the nanoparticles via covalent bond with amino groups.

Therefore, based on the concept of ROS utilization in cancer therapy, in sanitation, and in methods of modifying TiO₂ nanoparticles, the purpose of the present study was to apply the US/TiO₂ method to mammalian cell killing or injuring via ROS production. To achieve this goal, the ability of protein-modified TiO₂ nanoparticles targeted to specific tissues was investigated. In particular, the pre-S1/S2 protein, which is part of the L protein from hepatitis B virus²⁰ and recognizes hepatocytes, was immobilized on the surface of TiO₂ nanoparticles. Subsequently, the ability of the protein-modified TiO₂ nanoparticles to produce OH radicals was investigated.

Escherichia coli BL21(DE3) (Merck KGaA Novagen, Darmstadt, Germany) was used for the recombinant protein expression. The plasmids, pGEX-GFP-pre-S1/S2 and pGEX-GFP,²¹ were used for production of the fusion recombinant proteins, GST-GFP-pre-S1/S2 and GST-GFP, respectively. Using the production of GST-GFP-pre-S1/S2 as an example, a single colony of the transformant, harboring the pGEX-GFP-pre-S1/S2 plasmid, was inoculated into a test tube containing 3 ml of LB medium [1% (w/v) tryptone, 0.5% (w/v) yeast extract and 0.5% (w/v) NaCl] supplemented with 100 µg/ml ampicillin and incubated at 37 °C for 8 h with shaking (200 rpm). The culture medium (1 ml) was then seeded into a flask containing 200 ml LB medium with 100 µg/ml ampicillin, and incubated at 37 °C for approximately 3 h. When the absorbance at 600 nm of the culture medium reached 1.0 by spectrophotometer (U-3000, Hitachi, Tokyo, Japan), the cultivation temperature was decreased to 17 °C and IPTG was added to the culture medium at a final concentration of 0.1 mM for inducing of recombinant protein production. After 12 h of incubation, the cells were collected by centrifugation at 10,000g for 10 min, rinsed twice with running buffer (20 mM Hepes buffer (pH 8.0)), and suspended in 30 ml of running buffer containing 100 µg/ml PMSF as a protease inhibitor. The cytoplasmic fraction was extracted by ultrasonication on ice for 5 min (output = 100 W, duty = 40%, frequency = 20 kHz), and the supernatant was collected by centrifugation at 10,000g for 10 min. The pellet containing the inclusion body fraction was washed twice with 10 ml of wash buffer (20 mM Hepes, 0.5% (v/v) Triton X-100, and 1 mM EDTA, pH 8.0), re-suspended with folding buffer (20 mM Hepes, 1 mM DTT, and 1 mM EDTA) containing 8 M urea, and incubated at room temperature for 1 h. After centrifugation, the supernatant containing the denatured recombinant protein was dialyzed with folding buffer containing 4 M urea for 3 h at 4 °C. Subsequently, the supernatant was dialyzed with folding buffer containing 2 M urea for 3 h at 4 °C, and then dialyzed with folding buffer overnight at 4 °C. The sample then was centrifuged at 10,000g for 10 min, and the supernatant containing the recombinant GST-GFP-pre-S1/S2 protein was immobilized on PAA-TiO₂ nanoparticles as follow: Polyacrylic acid-modified TiO₂ particles (PAA-TiO₂, average diameter of 102 nm) were constructed as previously described¹⁸ using a MPT-422 TiO₂ suspension (Ishihara Sangyo Kaisha, Ltd, Osaka, Japan) as the starting material. GST-GFP-pre-S1/S2 and GST-GFP were immobilized onto the surface of the TiO₂ nanoparticles by chemical coupling at the carboxyl residue. The PAA-TiO₂ suspension (1.5% (w/v), 2.5 ml) was gently mixed with 0.5 ml of activating solution (0.2 M 1-ethyl-3-(3-dimethyl-aminopropyl)carbodiimide hydrochloride (ECD) and 0.05 M *N*-hydroxy succinimide (NHS)), and the mixture was incubated at room temperature for 1 h. Then, the PAA-TiO₂ suspension was applied to a PD-10 column (GE Healthcare Bio-Science AB, Uppsala, Sweden) to exchange the buffer solution for 20 mM HEPES buffer (pH 8.0), and remove un-reacted ECD and NHS. An eluted sample (3.5 ml) of the activated PAA-TiO₂ suspension was

mixed with 2.5 ml of the recombinant protein solution (approximately 1–2 mg/ml), and the mixture was incubated at 4 °C overnight. Subsequently, 1.0 ml of 0.1 M ethanolamine solution was added to block activated carboxyl residues and the mixture was incubated at 4 °C for an additional 30 min. The reacted mixture was separated using size exclusion chromatograph equipped with a AKTA FPLC (GE Healthcare Bio-Science AB, Uppsala, Sweden). In detail, 2.0 ml of sample was subjected to a Sephacryl S-500 HR column (16 × 300 mm, total bed volume 64 ml (GE Healthcare Bio-Science AB, Uppsala, Sweden)) that had been pre-equilibrated with 20 mM HEPES buffer (pH 7.4). Elution was performed with 0.5 ml/ml, and a sample was collected every 8 min (4 ml/tube). The size distribution of the protein-modified TiO₂ nanoparticles in each fraction was measured using a high performance particle sizer (HPP5001, Sysmex, Kobe, Japan). Immobilization of the recombinant protein on the TiO₂ nanoparticles was confirmed by surface plasmon resonance (SPR) analysis and sodium dodecyl sulphate polyacrylamide gel electrophoresis (SDS–PAGE). The weight of the TiO₂ particles was determined by the difference in particle weight before and after drying at 650 °C for 30 min. SPR analysis of the protein-modified TiO₂ nanoparticles was carried out using a BIACORE2000 (Biacore Life Sciences, Uppsala, Sweden). Anti-pre-S1 protein (80 µl) monoclonal antibody (0.5 mg/ml, Institute of Immunology Co., Ltd, Tokyo, Japan) was immobilized onto the CM-5 chip by chemical coupling with EDC and NHS according to the manufacturer's instruction manual. The interaction between GST-GFP-pre-S1/S2 protein-modified TiO₂ nanoparticles and the antibody was analyzed. The interactions of BSA-modified and unmodified TiO₂ nanoparticles with the antibody also were analyzed. In addition, for topographic observation of TiO₂ nanoparticles using atomic force microscopy (AFM), 10 µl of GST-GFP-pre-S1/S2 protein-modified TiO₂ nanoparticle suspension (0.002 % (w/v)) was dropped onto a cover glass (Matsunami, Japan) and dried under an air atmosphere. The topographic observation and average particle size analysis were performed using the dynamic force mode of AFM (SPA400 equipped with Nanonavi computer station, SIINT, Tokyo, Japan) with SI-DF20 as a cantilever.

Recombinant GST-GFP-pre-S1/S2 protein was recovered from the inclusion body fraction of cultivated transformant *E. coli* and refolded to form the soluble protein by dialyzing with folding buffers containing graded concentrations of urea (8 M to 0 M). The recovered sample was confirmed to be a single protein, approximately 72 kDa in size, by SDS–PAGE analysis (data not shown), and the purified protein concentration was estimated to be 2.98 mg/ml using the Bradford method. The GST-GFP-pre-S1/S2 protein was immobilized on the surface of the TiO₂ nanoparticles (average diameter 102 nm, see Table 1) by chemical coupling between the terminal amino group of the protein and the terminal carboxyl group of polyacrylic acid. The protein-modified TiO₂ nanoparticles were purified by size exclusion chromatography. The protein-modified TiO₂ nanoparticle suspended in 20 mM HEPES buffer was eluted in the void fraction and was completely separated from the unbound free protein (data not shown). The protein-modified TiO₂ nanoparticle suspension was stable in culture medium for at least 2 days (Table 1), although there was slight

Table 1
Average particle size of GST-GFP-pre-S1/S2-modified TiO₂ nanoparticles

Particle type	Average size (nm)
PAA-TiO ₂	102
GST-GFP-pre-S1/S2 immobilized TiO ₂ (immediately)	120 ^a
GST-GFP-pre-S1/S2 immobilized TiO ₂ (after 1 day)	136 ^a
GST-GFP-pre-S1/S2 immobilized TiO ₂ (after 2 days)	174 ^a

^a The particle size distribution analysis was performed after re-suspension in DMEM.

particle aggregation after static incubation at 4 °C. Furthermore, AFM analysis of GST-GFP-pre-S1/S2-modified TiO₂ nanoparticles showed protein-modified TiO₂ nanoparticles were of similar diameter (Fig. 1), and the average particle size based on topographic measurements was estimated to be 152 nm (data not shown). Each evaluation result was well agreed, and strongly indicated that the protein-modified TiO₂ nanoparticle form 100 to 150 nm scale size nanoparticle without particle aggregation. The molecular interaction between the anti-preS1 antibody and the protein-modified TiO₂ nanoparticles was investigated using a SPR sensor. First, a solution of free GST-GFP-pre-S1/S2 protein was applied to a CM-5 chip coated with anti-pre-S1 antibody equipped with BIACORE2000 (Fig. 2A). The resonance unit was increased in a dose-dependent manner and the antibody immobilized on the chip recognized pre-S1 protein. Next, GST-GFP-pre-S1/S2-modified TiO₂ nanoparticles were applied to the same chip (Fig. 2B). Although the immobilized protein concentration of the TiO₂ nanoparticle suspension was 0.8 µM, a significant interaction was observed. As a control, TiO₂ nanoparticles were modified with the same concentration of bovine serum albumin (BSA); there was no significant increase in the resonance unit. Therefore, it was concluded that the GST-GFP-pre-S1/S2 protein was covalently bound by chemical coupling to the surface of the TiO₂ nanoparticles without any denaturation of the protein.

Human hepatoma HepG2 cells were cultured in Dulbecco's modified Eagle medium (DMEM, Nakarai Tesqu, Kyoto, Japan), supplemented with 10% (v/v) fetal bovine serum (FBS; Invitrogen GIBCO, Carlsbad, CA, USA), 60 µg/ml penicillin (Nakarai Tesqu, Kyoto, Japan), and 100 µg/ml streptomycin (Nakarai Tesqu, Kyoto, Japan). The cells were maintained at 37 °C and under a 5% CO₂ atmosphere. Approximately 2×10^5 HepG2 cells, counted by hemacytometer, suspended in 2 ml DMEM were seeded in 35-mm culture dishes and incubated for 24 h. Then, the recombinant protein-modified TiO₂ nanoparticles suspension were added to the culture medium at a final concentration of 0.01% (w/v) (=0.1 g/l) of TiO₂ and cultured for an additional 6 h because it was reported about the complete uptake of BNC was attained within 6 h in HepG2.²⁰ After additional cultivation, the culture dishes were washed twice with 500 µl of PBS(–) buffer. To immobilize the cells, 500 µl paraformaldehyde (PFA) solution (4%) was added to the dish, followed

by incubation at room temperature for 15 min. After removal of the PFA solution, cells were permeabilized with 500 µl of 0.25% (w/v) Triton X-100 in PBS(–) buffer for 15 min. Then, the primary antibody solution (500 µl of 1 µg/ml anti-pre-S1 or 4.4 µg/ml anti-GFP monoclonal antibody (Nakarai Tesqu, Kyoto, Japan)) in PBS(–) buffer was added to the dish, followed by an overnight incubation at 4 °C. After washing three times with 0.03% (w/v) Triton X-100 in PBS(–) buffer, the secondary antibody solution (500 µl, 4 µg/ml Alexa Fluor 555 goat anti-mouse IgG antibody (Invitrogen, Carlsbad, CA, USA)) was added to the dish, followed by incubation at room temperature for 1 h. After washing three times with 0.03% (w/v) Triton X-100 in PBS(–) buffer, uptake of protein-modified TiO₂ nanoparticles by HepG2 cells was observed using a fluorescent microscope (BZ-8000, KEYENCE, Osaka, Japan). After incubation of HepG2 cells with protein-modified TiO₂ nanoparticles for 6 h, the uptake of TiO₂ nanoparticles was observed by fluorescent microscopy (Fig. 3). Cell morphology was unchanged by incubation with TiO₂ nanoparticles (Fig. 3A, C, G, and I) or with free protein (Fig. 3B and H). Free GST-GFP-pre-S1/S2 protein recognized HepG2 cells, and its clearance was nearly complete after a 6-h incubation period (Fig. 3E and K). The uptake of GST-GFP-pre-S1/S2-modified TiO₂ nanoparticles also was observed by staining with anti-preS1 and anti-GFP monoclonal antibodies (Fig. 3D and J). The fluorescence signal was observed proximal to the cell membrane. The GST-GFP-pre-S1/S2-modified TiO₂ nanoparticles appeared to adhere to the cell membrane, but did not translocate into the cytosol fraction. As a negative control, the uptake of GST-GFP-modified TiO₂ nanoparticles also was investigated (Fig. 3F and L); there was no evidence of GST-GFP-modified TiO₂ nanoparticle uptake. In addition, there was no evidence of non-specific endocytosis of TiO₂ nanoparticles by HepG2 cells (Fig. 3L). Based on these observations, it was assumed that the GST-GFP-pre-S1/S2-modified TiO₂ nanoparticles specifically recognized the HepG2 cells.

Aminophenyl fluorescein (APF, Daiichi Pure Chemicals Co., Ltd, Tokyo, Japan) was used to quantify OH radicals. The APF solution (1 µM) was prepared with PBS(–) buffer. APF solution (2 ml) was added to each dish, and subsequently, protein-modified TiO₂ nanoparticles were added at a final concentration of 0.01% (w/v). Then, each dish was irradiated with high frequency ultrasound (1 MHz) at intensity varied between 0 and 2.0 (W/cm²) for 30 s. The amount of fluorescein generated from the reaction of APF with OH radicals was measured using a multi-well plate reader CytoFluor 4000 (Applied Biosystems, Foster City, CA, USA) at an excitation wavelength of 490 nm and an emission wavelength of 515 nm. OH radical generation from both rutile and anatase TiO₂ particles using ultrasound irradiation has been confirmed.⁸ This method has been established for killing of various microorganisms, such as *E. coli* and *Legionella*.^{11–13} Based on these previous findings and on the targeting potential of protein-modified TiO₂ nanoparticles, effective cell injuring using the combination of ultrasound irradiation and TiO₂ nanoparticles was investigated. First, the OH radical generation ability of TiO₂ nanoparticles in the absence of cultured cells was measured by high frequency ultrasound irradiation (1 MHz) (Fig. 4). Although ultrasound irradiation itself has OH radical-generating potential, the additional PAA-TiO₂ nanoparticles enhanced OH radical production 1.3–1.5-fold at intensity of 0.4 W/cm². In addition, the capacity of protein-modified TiO₂ nanoparticles to generate OH radicals exhibited the same response (data not shown). Therefore, it was assumed that PAA-TiO₂ nanoparticles had the potential to generate OH radicals.

For evaluating of cell injury resulting from the combination of TiO₂ nanoparticles and ultrasound irradiation, after incorporating protein-modified TiO₂ nanoparticles, HepG2 cells were washed three times with fresh DMEM (2 ml) and were then re-suspended in 2 ml DMEM. Ultrasound irradiation was performed as follows:

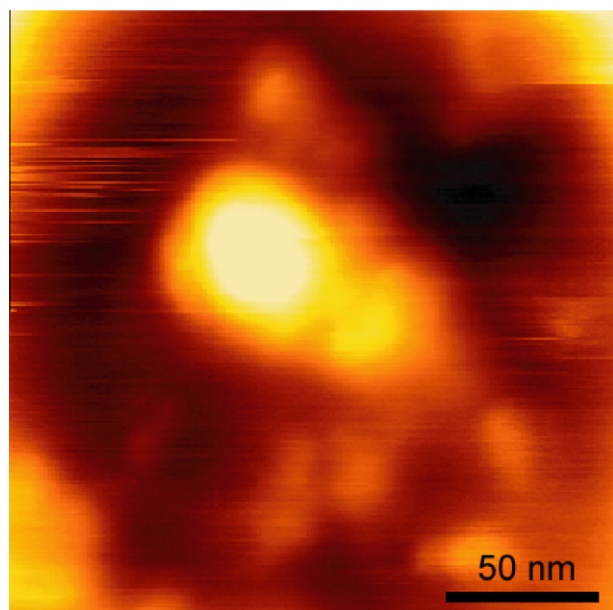


Figure 1. Topographic observation of GST-GFP-pre-S1/S2-modified TiO₂ nanoparticles using AFM. Scale bar indicates 50 nm.

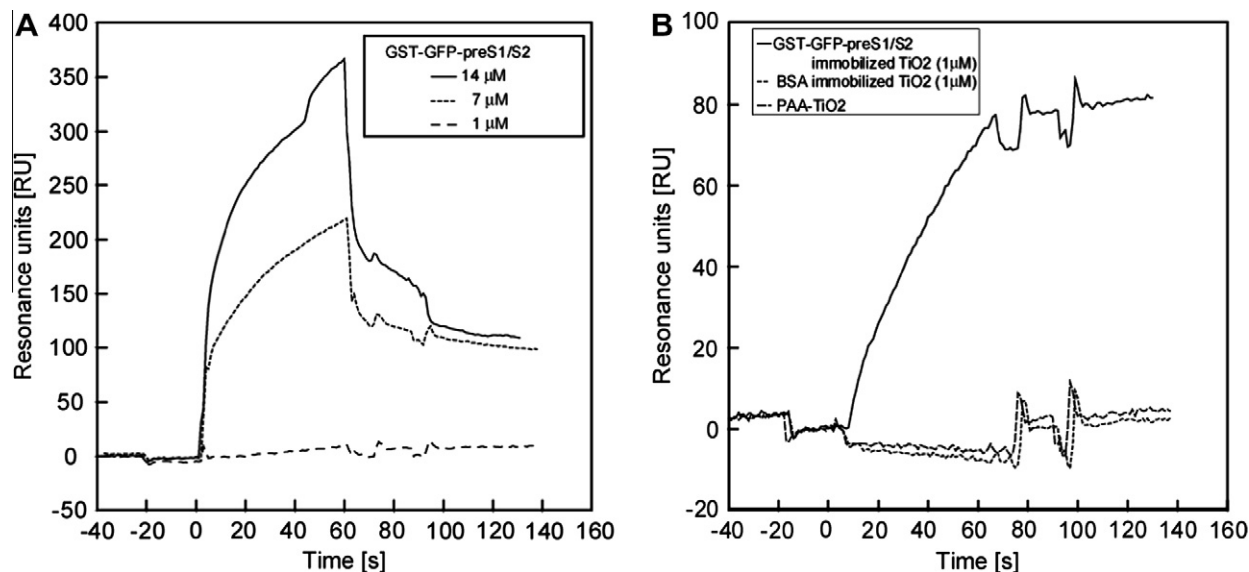


Figure 2. Confirmation of GST-GFP-preS1/S2 immobilization on the surface of TiO₂ nanoparticles. The sensorgram of free GST-GFP-preS1/S2 (A) and GST-GFP-preS1/S2-modified TiO₂ nanoparticles (B) using anti-preS1 antibody was analyzed using BIACORE2000.

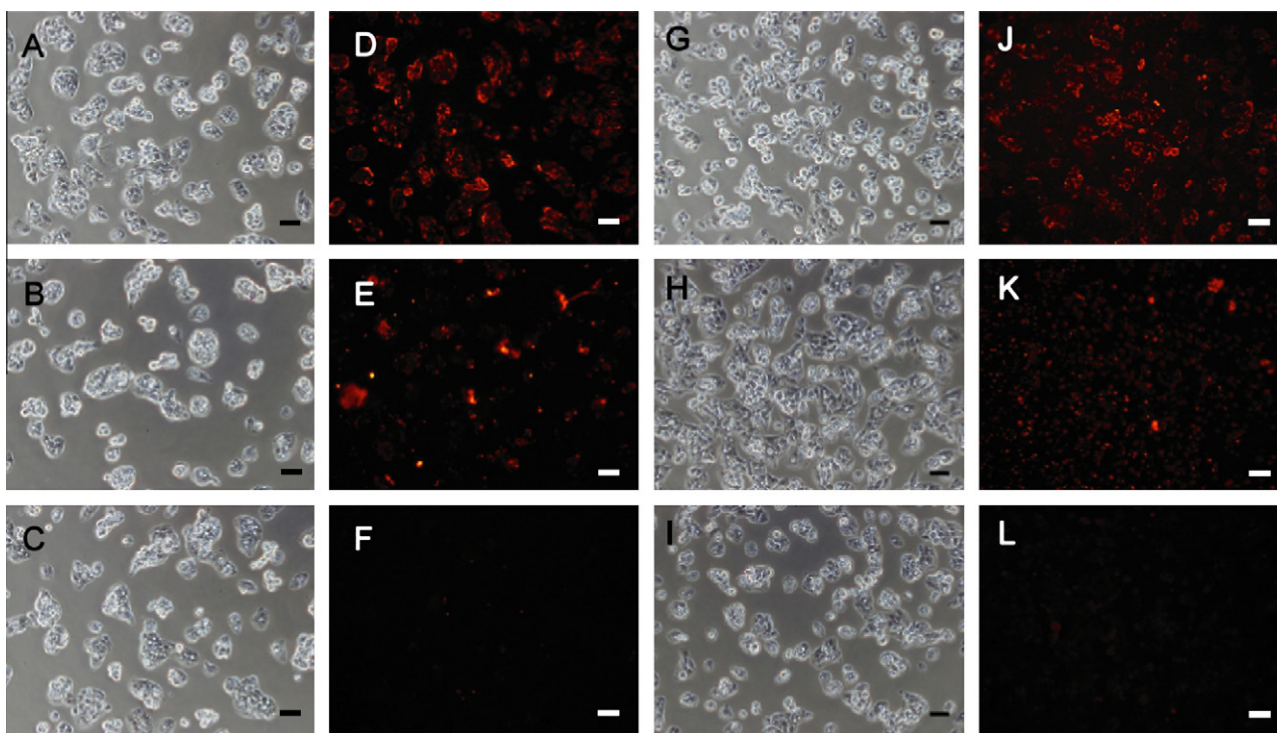


Figure 3. Immuno-staining of HepG2 for uptake of GST-GFP-preS1/S2-modified TiO₂ nanoparticles. The uptake of GST-GFP-preS1/S2-modified TiO₂ nanoparticles (A, D, G, J), free GST-GFP-preS1/S2 protein (B, E, H, K) and GST-GFP-modified TiO₂ nanoparticles (C, F, I, L) was confirmed by fluorescent microscopy after staining with anti-preS1 monoclonal antibody (A–F) and anti-GFP monoclonal antibody (G–L), respectively. Phase-contrast images are shown in panels A–C and G–I and fluorescent images are presented in panels D–F and J–L. Each scale bar indicates 50 μ m.

frequency, 1 MHz; duty, 50%; and, irradiation time, 30 s. After irradiation, lactose dehydrogenase (LDH) activity leaked from damaged cells into the culture medium was measured using a CytoTox-One homogeneous membrane integrity assay kit (Promega, Madison, WIS, USA). In brief, the fluorescence intensity of the final product, resorufin, which is produced by a sequential reaction involving LDH, was measured using a multi-well plate reader, CytoFluor 4000, at an excitation wavelength of 560 nm and an emission wavelength of 590 nm. Cell-injury was performed using the US/TiO₂ method and cell damage was monitored by measuring

the amount of LDH that leaked out of the cell (Fig. 5). At 0.6 W/cm², the fluorescent intensities, which were indicative of leaked LDH, were saturated in each experimental condition; therefore, it was assumed that most cells were killed. In contrast, there were no significant differences among the three conditions at intensity of 0.2 W/cm². Therefore, this irradiation intensity was deemed insufficient for significant cell injury, as OH radicals were not generated under this condition (Fig. 4). At an irradiation intensity of 0.4 W/cm², LDH leakage was subsequently increased by addition of TiO₂ nanoparticles, and LDH activity was saturated in the

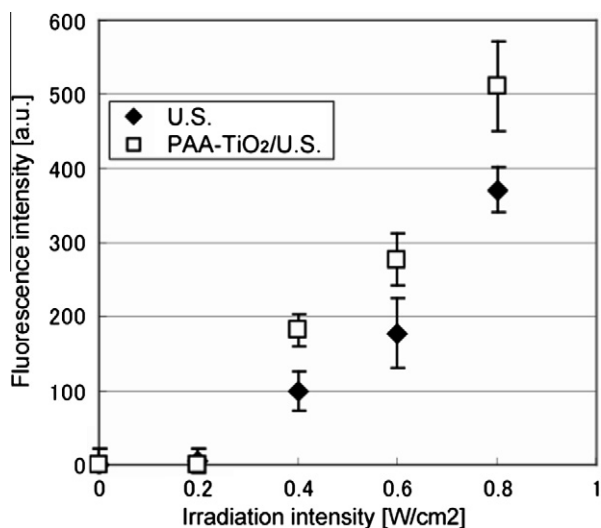


Figure 4. Measurement of OH radical generation by modified TiO₂ nanoparticles as a result of high frequency ultrasound irradiation. Generation of OH radicals was measured using ultrasonic irradiation with PAA-TiO₂ (open box) and without any particle (close diamond). Data are the mean of six independent experiments, and the error bar indicates the standard deviation.

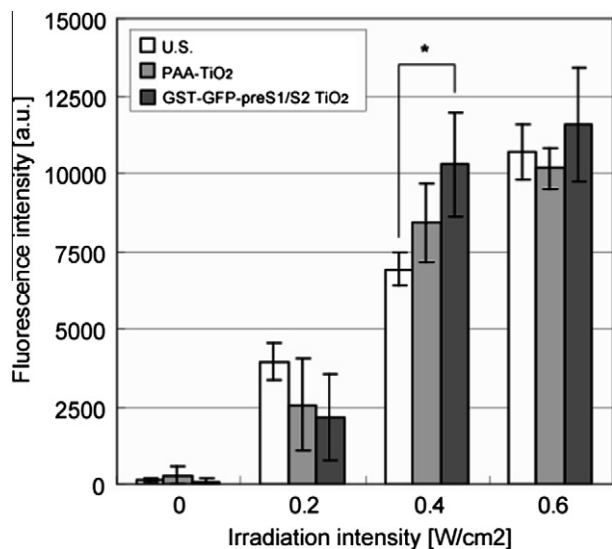


Figure 5. Membrane injury in HepG2 cells as a result of the combination of TiO₂ nanoparticles and ultrasound irradiation. LDH leaked from cells as a result of membrane injury was measured. Data are the mean of seven independent experiments, and the error bar indicates the standard error. Significant difference between groups ($p < 0.05$, one-way ANOVA).

presence of GST-GFP-pre-S1/S2-modified TiO₂ nanoparticles. Based on these results, it was assumed that TiO₂ nanoparticles localized to HepG2 cells as a result of the pre-S1/S2 protein-enhanced OH radical generation, thereby injuring the cells.

The PAA-TiO₂ nanoparticles were approximately 100 nm in diameter; protein-modification increased particle diameter (Table 1). The increment in diameter was 20 nm, and it was assumed that the increased length was equivalent to the sum of the diameters of two protein molecules, as immobilized protein covered the TiO₂ nanoparticles in a single layer. Based on the theory of Flory, the diameter of GST-GFP-pre-S1/S2 was estimated to be 7 nm;²² therefore, the increased diameter of the nanoparticles was consistent with this theoretical estimate. The number of protein molecules immobilized on each TiO₂ nanoparticle was estimated to be 420

using the following parameters: average diameter of each TiO₂ nanoparticle, 100 nm; protein concentration of GST-GFP-pre-S1/S2, 64 mg/L; TiO₂ nanoparticle concentration, 3 g/L; specific gravity of TiO₂ nanoparticles, 4.5 g/cm³; and, the putative globule diameter of GST-GFP-pre-S1/S2 protein, 10 nm. The theoretical values for these parameters were as follows: number of protein molecules per nanoparticle, approximately 440; putative globule protein diameter, 10 nm; and, nanoparticle diameter, 100 nm. Applying these theoretical values to TiO₂ nanoparticles covered with a single layer of protein molecules, there was good agreement between the measured and theoretical number of protein molecules per nanoparticle. The theoretical estimates suggest that the surface of TiO₂ nanoparticles was completely covered with protein molecules.

The GST-GFP-pre-S1/S2 protein displayed on the surface of the TiO₂ nanoparticles was recognized by the anti-preS1 antibody (Fig. 2B), and allowed the nanoparticles to be localized to the HepG2 cells (Fig. 3D and J). Moreover, the protein-modified TiO₂ nanoparticles were capable of OH radical generation even though the particle surface was covered with protein (Fig. 4). Based on these results, it was concluded that the protein-modified TiO₂ nanoparticles have a dual function: targeting TiO₂ nanoparticles to specific cells and generating OH radicals that result in cell injury. The GST-GFP-pre-S1/S2-modified TiO₂ nanoparticles were localized in the vicinity of the cell membrane (Fig. 3D and J), while the free GST-GFP-pre-S1/S2 protein translocated to the cytosol (Fig. 3E and K). Although the fusion between hepatitis B virus and liver cells was complete after 6 h in a previous study,²⁰ only partial fusion occurred between the nanoparticles and HepG2 cells in this study. Therefore, it was assumed that the protein-modified nanoparticles cannot be cleared by endocytosis.

Ultrasound irradiation at intensity of 0.4 W/cm² and a frequency of 1 MHz to HepG2 cells that had incorporated TiO₂ nanoparticles resulted in cell damage (Fig. 5). The number of OH radicals generated in the presence of TiO₂ nanoparticles at 0.4 W/cm² was equivalent to that at 0.6 W/cm² in the absence of TiO₂ nanoparticles (Fig. 4). Therefore, it was assumed that cell damage could be induced by these OH radical concentrations, regardless of the experimental conditions. Because the high ultrasound irradiation intensity could be damage to the TiO₂ non-delivered cell, a comparable lower intensity should be required for target cell damaged irradiation. There are several possible ways to improve cell damage efficiency at lower ultrasound irradiation intensity as follows: enhance the immobilization efficiency of GST-GFP-pre-S1/S2 protein to the TiO₂ nanoparticles; improve, either directly or indirectly, the ultrasound irradiation method; and change the frequency of ultrasound irradiation. Furthermore, the combination of ultrasound and ultraviolet irradiation could be gain an advanced improvement of irradiation efficiency. In addition, the mechanism of cell injury that occurs as a result of the US/TiO₂ method warrants investigation, as it has not been studied.

As a conclusion, this is the first study demonstrating the use of TiO₂ nanoparticles to cause cell-specific damage. The protein-modification in the TiO₂ nanoparticles served the dual functions of specific cell-recognition and OH radical generation. Modification of TiO₂ nanoparticles with various targeting proteins, such antibodies or epidermal growth factor (EGF), will allow this method to be used to target specific cancer cells. Furthermore, the combination of ultrasound irradiation and TiO₂ nanoparticle will be an alternative targeted tissue specific cancer cell treatment methodology such like a PDT in the near future.

Acknowledgments

This work was supported, in part, by a Grant-in-aid from the Ministry of Education, Culture, Sports, Science and Technology, Japan (Nos. 18650143 and 18015019 to N.S.).

References and notes

1. Fujishima, A.; Honda, K. *Nature* **1972**, 238, 37.
2. Fujishima, A.; Rao, T. N.; Try, D. A. *J. Photochem. Photobiol. C* **2000**, 1, 1.
3. Christensen, P. A.; Curtis, T. P.; Egerton, T. A.; Kosa, S. A. M.; Tinlin, J. R. *Appl. Catal., B* **2003**, 41, 371.
4. Bekbolet, M. *Water Sci. Technol.* **1997**, 35, 95.
5. Cai, R.; Kubota, Y.; Shuin, T.; Sakai, H.; Hashimoto, K.; Fujishima, A. *Cancer Res.* **1992**, 52, 2346.
6. Kubota, Y.; Shuin, T.; Kawasaki, C.; Hosaka, M.; Kitamura, H.; Cai, R.; Sakai, H.; Hashimoto, K.; Fujishima, A. *Br. J. Cancer* **1994**, 70, 1107.
7. Fujishima, A.; Zhang, X. *C.R. Chim.* **2006**, 9, 750.
8. Shimizu, N.; Ogino, C.; Dadjour, M. F.; Murata, T. *Ultrason. Sonochem.* **2007**, 14, 184.
9. Harada, H. *Ultrason. Sonochem.* **2001**, 8, 55.
10. Berberidou, C.; Poullos, I.; Xekoukoulotakis, N. P.; Mantzavinos, D. *Appl. Catal., B* **2007**, 74, 63.
11. Dadjour, M. F.; Ogino, C.; Matsumura, S.; Shimizu, N. *Biochem. Eng. J.* **2005**, 25, 243.
12. Dadjour, M. F.; Ogino, C.; Matsumura, S.; Nakamura, S.; Shimizu, N. *Water Res.* **2006**, 40, 1137.
13. Ogino, C.; Dadjour, M. F.; Takaki, K.; Shimizu, N. *Biochem. Eng. J.* **2006**, 32, 100.
14. Szeimies, R. M.; Landthaler, M. *Recent Results Cancer Res.* **2002**, 160, 240.
15. Silva, J. N.; Filipe, P.; Morliere, P.; Maziere, J. C.; Freitas, J. P.; Cirne, d. e.; Castro, J. L.; Santus, R. *Biomed. Mater. Eng.* **2006**, 16, 147.
16. Roots, R.; Okada, S. *Radiat. Res.* **1975**, 64, 306.
17. Chadwick, M. D.; Goodwin, J. W.; Lawson, E. J.; Mills, P. D. A.; Vincent, B. *Colloids Surf., A* **2002**, 203, 229.
18. Kanehira, K.; Banzai, T.; Ogino, C.; Shimizu, N.; Kubota, Y.; Sonezaki, S. *J. Colloid Interface Sci.* **2008**, 64, 10.
19. Pettersson, A.; Marino, G.; Pursiheimo, A.; Rosenholm, J. B. *J. Colloid Interface Sci.* **2000**, 228, 73.
20. Yamada, T.; Iwasaki, Y.; Tada, H.; Iwabuki, H.; Chuah, M. K.; VandenDriessche, T.; Fukuda, H.; Kondo, A.; Ueda, M.; Seno, M.; Tanizawa, K.; Kuroda, S. *Nat. Biotechnol.* **2003**, 21, 885.
21. Kasuya, T.; Yamada, T.; Ueda, A.; Matsuzaki, T.; Okajima, T.; Tatematsu, K.; Tanizawa, K.; Kuroda, S. *J. Biosci. Bioeng.* **2008**, 106, 99.
22. Flory, P.J. Cornell University Press: Ithaca, NY, 1953.